International Journal Multidisciplinary
Homepage : https://journal.antispublisher.com/index.php/IJMI
Email : admin@antispublisher.com

e-ISSN : 3031-9870
IJMI, Vol. 3, No. 2, May 2026
Page 432-445

Computational DFT Analysis of Monocarbonyl Curcumin and Pyrazole Derivatives: Molecular Geometry, Electrostatic Surface Potential, Electronic Transition Spectra, and Mulliken Charges

Hayder S. Mahdi [1], Tahseen A. Alsalim [2]
[1,2] University of Basrah, Iraq

DOI : https://doi.org/10.61796/ijmi.v3i2.486

Sections Info

Article history:
Submitted: February 07, 2026
Final Revised: March 21, 2026
Accepted: April 08, 2026
Published: May 15, 2026

Keywords:
MCC
pyrazole
DFT
B3LYP
Vibration
Mulliken Charges
HOMO
LUMO

ABSTRACT

Objective: *Monocarbonyl curcumin (MCC) analogues and those of pyrazole derivatives were investigated in their structural and electronic features.* ***Method:*** *Applying the Density Functional Theory (DFT) at B3LYP/6-311G++(d,p) level, it is examined molecular geometry, electrostatic surface potential (ESP), frontier molecular orbitals (FMO), and Mulliken charges.* ***Results:*** *Results show that although MCC compounds have a near-planar structure, the pyrazole derivatives develop non-planar geometries. Electronic absorption spectra, based on TD-DFT, display prominent transitions in UV-visible areas, where compound BPY yielded the lowest transition energy gap (2.8774 eV) and maximum absorption wavelength (λ_{max} = 430.89 nm).* ***Novelty:*** *The results imply the effect of the formation of pyrazole rings on electronic delocalization and charge transfer characteristic and provide knowledge for designing more stable and biologically active curcumin-based heterocyclic systems.*

INTRODUCTION

Curcumin (diferuloylmethane), a naturally occurring polyphenolic component derived from the rhizomes of Curcuma longa, has attracted considerable interest due to its wide pharmacological activity, including antioxidant, antiviral, anticancer, anti-inflammatory, and antimicrobial activities [1], [2], [3]. Moreover, curcumin holds tremendous therapeutic value in neurodegenerative disorders, cardiovascular diseases, and metabolic syndromes owing to its capacity to regulate various cellular signaling mechanisms [4], [5]. Although curcumin has several potential biological roles, few of these are available for clinical or pharmacological applications due to its poor aqueous solubility, rapid metabolism, low bioavailability, and chemical instability in physiological conditions [6]. It is believed that the β-diketone moiety in the curcumin structure predominantly accounts for its instability and rapid degradation in biological media [7], [8]. For these limitations, a great effort has been done in the synthesis and design of monocarbonyl curcumin analogues (MACs) (i.e., monocarbonyl linkers, replacing β-diketone group) [6], [9]. This structural modification greatly enhances chemical stability, pharmacokinetic characteristics and biological activity without losing the conjugated framework responsible for a pharmacological profile of curcumin derivatives [10], [11]. Diverse biological activities of monocarbonyl curcumin in antibacterial, anticancer, antioxidant, anti-inflammatory, antimalarial and antitubercular activities are reported as their derivatives [9], [12]. In addition, the insertion of electron-

donating or electron-withdrawing substituents in the aromatic rings significantly alters the electronic distribution, molecular reactivity and biological activity of these compounds [11], [13]. One of the nitrogen-containing five-membered heterocycles and one of the most popularly used compounds in the field of medicinal chemistry and material science are those derivatives of pyrazole [14], [15]. Pyrazole derived compounds carry a range of biological properties such as: antimicrobial, analgesic, anti-inflammatory, antioxidant, anticonvulsant or anticancer properties [16], [17]. Due to their favorable electronic properties and high pharmacological activity, pyrazole analogues are attractive scaffolds for their use as biologically active compounds [18]. The use of the pyrazole ring as monocarbonyl curcumin analogues is also successful in enhancing the molecular stability, biological activity, and electronic delocalization [19], [20]. Pyrazole formation due to cyclization alters the conjugated electronic system and influence the molecular geometry, charge transfer relations and optical behavior of the obtained derivatives [21], [22]. As a result, pyrazole-functionalized monocarbonyl curcumin compounds possess more robust cytotoxic, antioxidant and spectroscopic activities than their original kinetics counterparts [23]. According to this view, DFT calculations offer robust and reliable computational methods for chemical evolution of organic and heterocyclic compounds [24], [25] in the past years. DFT methods are able to yield theoretical data on optimized molecular geometry, total energy, dipole moment, vibrational frequencies, molecular electrostatic potential, frontier molecular orbitals as well as many other variables [26], [27]. Frontier molecular orbitals, especially the highest occupied molecular orbital (HOMO) and lowest unoccupied molecular orbital (LUMO), are a major class of molecular stability, chemical reactivity, intramolecular charge transfer, and non-linear optical property characterization [28], [29]. The energy gap of HOMO–LUMO is often used as an indicator of kinetic stability and electronic excitation characteristics of molecular systems [30]. Furthermore, Mulliken atomic charge analysis has been utilized for prediction of charge distribution and selection of electron-rich and electron deficient area in the molecules that are significant in intermolecular interactions and biological activity [31], [32]. Likewise, theoretical vibration spectral calculations using DFT methodologies offer an accurate corroboration for direct assignment and interpretation of FT-IR and Raman spectra [33]. Accordingly, our objective in this paper is the theoretical DFT evaluation of monocarbonyl curcumin compounds (A, B, C, and D) and pyrazole derivatives (APY, BPY, CPY, and DPY) (Figure 1) to appraise their molecular structures and electronic characteristics, vibrational spectra, as well as Mulliken charge distributions. The theoretical conclusions obtained by combining these results should provide more detailed indications about the structure–property linkages and physicochemical behaviour of these biologically important heterocyclic systems.

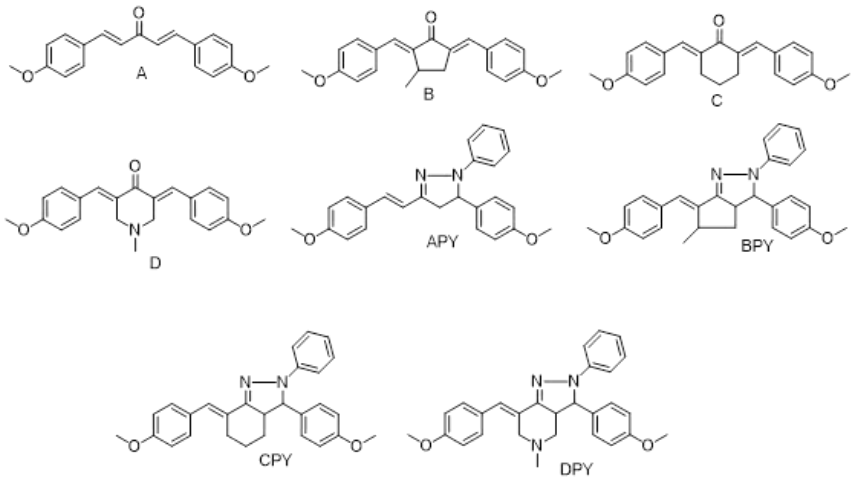

Figure 1. The 2D structure of studied compounds

RESEARCH METHOD

The structures of the studied compounds are presented in GaussView 6. For geometry optimization and frequency calculations, Gaussian 09 [34] was used to implement geometrical optimization and frequency calculation in the gas phase. Density functional theory (DFT) [13] and the Becke-style three-parameter functional with Lee-Yang-Parr exchange-correlation functional (B3LYP) method [35] were used to optimize the structures of MCC and pyrazole compounds. 6-311G++(d,p) was employed for atomic orbitals. Frequency calculations were performed after geometry optimizations, and no imaginary frequency was found. EHOMO and ELUMO are found as the frontier molecular orbital energies by using the same level of study.

RESULTS AND DISCUSSION

The geometric structure Analysis

The electronic character and physicochemical properties of attached substituents can have a significant influence on the geometry and physicochemistry of the synthesized compounds, such as charge distributions, dipole moments, the energy gap (ΔE) between frontier molecular orbitals (FMOs), and their overall molecular stability. The electronic effect of substituents on reaction mechanism and rate is significantly determined by dipole moment, molecular polarity, and optimized geometry [36]. In this paper, we utilize the density functional theory (DFT) applied at the B3LYP level with the 6-311G++(d,p) basis set in the gas phase to obtain the optimized geometric structures of the studied molecules. The analytical results demonstrated that all the MCC compounds were classified with respect to molecular structure of close to planar characters and that the pyrazole compounds are not planar. However, differences to the planar structure were observed with different ketone structure of the MCC derivatives. The optimal shapes of the investigated molecules are shown in Figure 2.

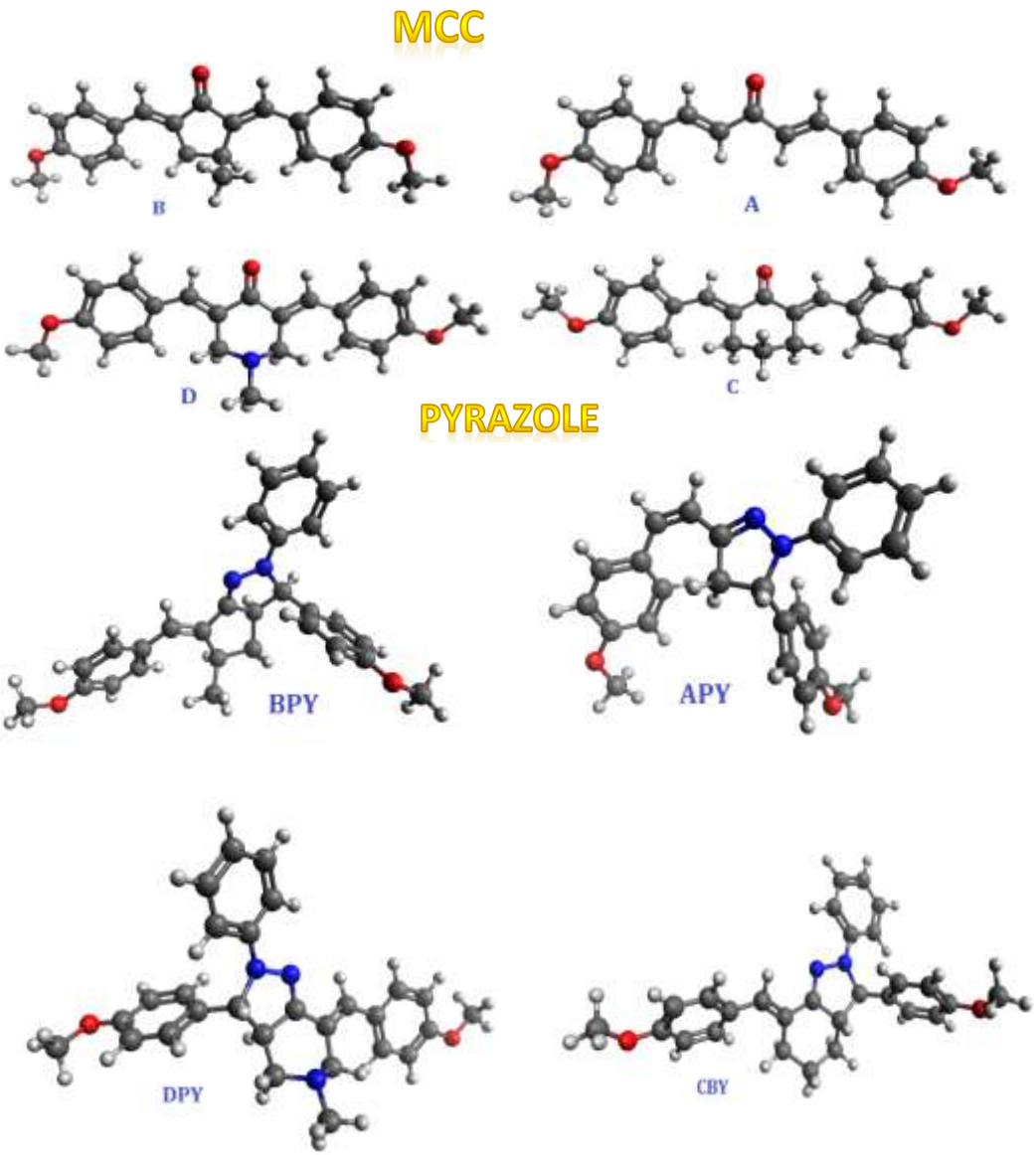

Figure 2. The 3D structures of MCC and pyrazole compounds.

Analyzing the electrostatic surface potential.

ESP mapping illustrates the electron-rich (negative) and electron-poor (positive) regions of molecules (Figure 3). The red areas correspond to high electron density, while the blue areas correspond to electron-deficient regions [37], [38], [39]. Compounds A–D exhibit considerable variations in MEP measurement electron distribution, fundamentally influencing their NLO and biological properties. Compound A has a symmetric MEP that gives a strong negative carbonyl oxygen and moderately positive β-protons, leaving a weak donor–acceptor polarization, thus with weak ICT. Compound B demonstrates a higher electrostatic asymmetry, which can promote charge separation relative to compound A, and compound C presents a diffuse and weakly polarized MEP owing to the chair conformation of cyclohexanone, so that the aromatic rings are distorted from planarity and therefore impair charge separation. In compound C, where only positively and negatively interspersed regions overlap, a lower dipole moment occurs

and inhibits the ICT, thus generating weak NLO and also low biological activity. Compound D possesses an optimal electrostatic composition with very strong negative piperidine nitrogen and carbonyl oxygen atoms being located well away from the positive (aliphatic) regions. The donor–π–acceptor configuration gives the highest possible charge separation, and the highest potential difference. MCC compounds, as pyrazole derivatives, have a chemical composition that includes electron density redistribution with the replacement of the carbonyl by C=N moiety. APY retains molecular planarity and ICT by extending conjugation, resulting in large hyperpolarizability with similar effects to compound D. BPY is characterized by reduced NLO due to electrostatic clutter and ring fusions that may have an effect on orbital alignment. CPY features the lowest donor–acceptor separation and the most diffuse MEP with the lowest hyperpolarizability and low biological activity. DPY has a semi-donor character but weakened conjugation continuity and acceptor strength, which further reduces NLO response and binding affinity. Overall, relatively strong NLO functions and biological functions are responsible for good donor–acceptor separation and molecular planarity, plus prolonged π-conjugation, and are exhibited predominantly for compounds D and APY.

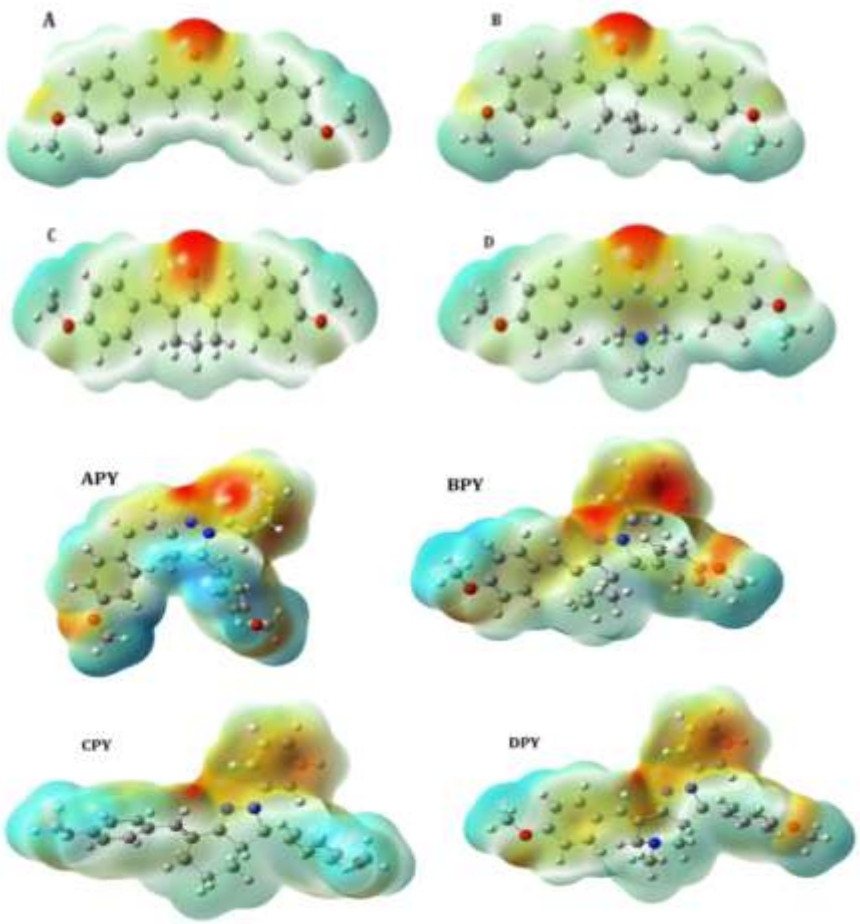

Figure 3. The ESP diagram of studied compounds (A, B, C, D, APY, BPY, CPY, and DPY) at the DFT/B3LYP level of theory with the bases set to 6-311G++(d,p).

Mulliken atomic charge analyses for the studied compounds.

The Mulliken atomic charge analysis detected large electron-density redistribution of the monocarbonyl curcumin compounds and their pyrazole derivatives [40, 41]. For the compound A, the largest positive charges were found at C4 (+1.5237) and C21 (+1.3767) and the lowest were found at C22 (−0.8988) and C3 (−0.8536). The subsequent addition of pyrazole in APY balanced the charge distribution, making C4 (+1.3012) more positive in center position and C24 (−0.8688) the more negative site. In compounds B, C, and D, the oxygen atoms had the greatest number of negative charge (O34 (−0.5354) in B, O37 (−0.5376) in C, and O30 (−0.5369) in D), indicating an extremely electron rich character (Figure 4). The pyrazole nitrogen atoms of the pyrazole derivatives BPY, CPY, and DPY were the most negative-charged N28 (−0.6571), N48 (−0.6164) and N25 (−0.6127), while positive charges were found predominantly on the carbon atoms and included C34 (+0.3679), C54 (+0.3223) and C40 (+0.3204) (Figure 5). In general, Mulliken charge information reveals that the oxygen and nitrogen heteroatoms are the predominant electron rich centers in all species to be studied and only several other carbon atoms in conjugated systems are positively polarized. The addition of pyrazole rings generally facilitated charge separation and led to electron delocalization suggesting that heterocyclic substitution exerted a strong effect on the electronic characteristics of the monocarbonyl curcumin compounds.

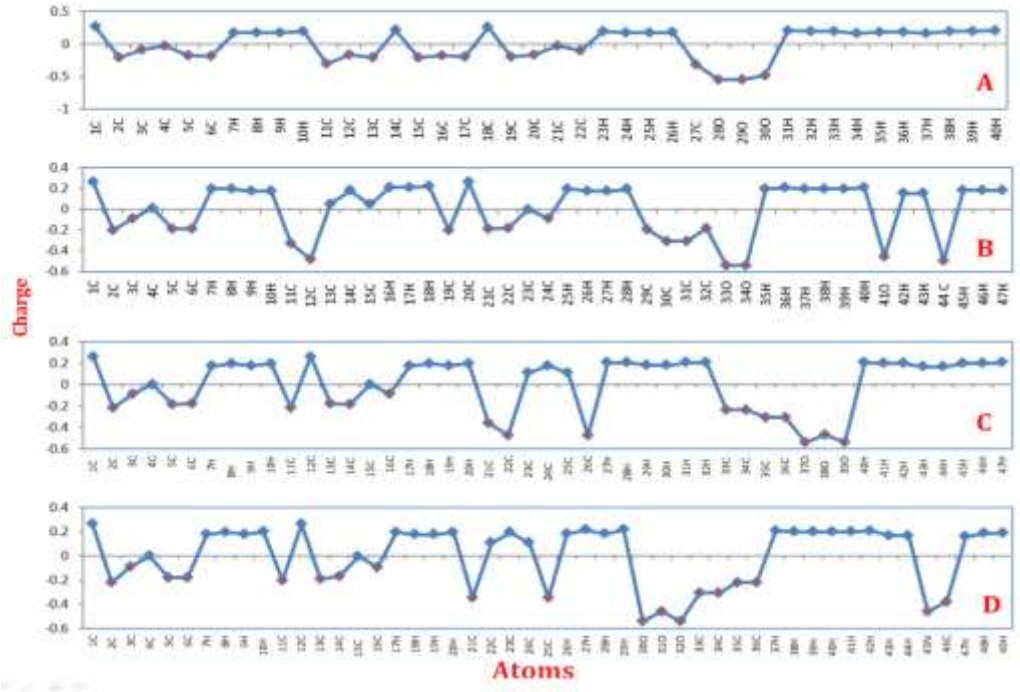

Figure 4. The atomic charge distribution according to Mulliken of MCC compounds (A, B, C, and D)

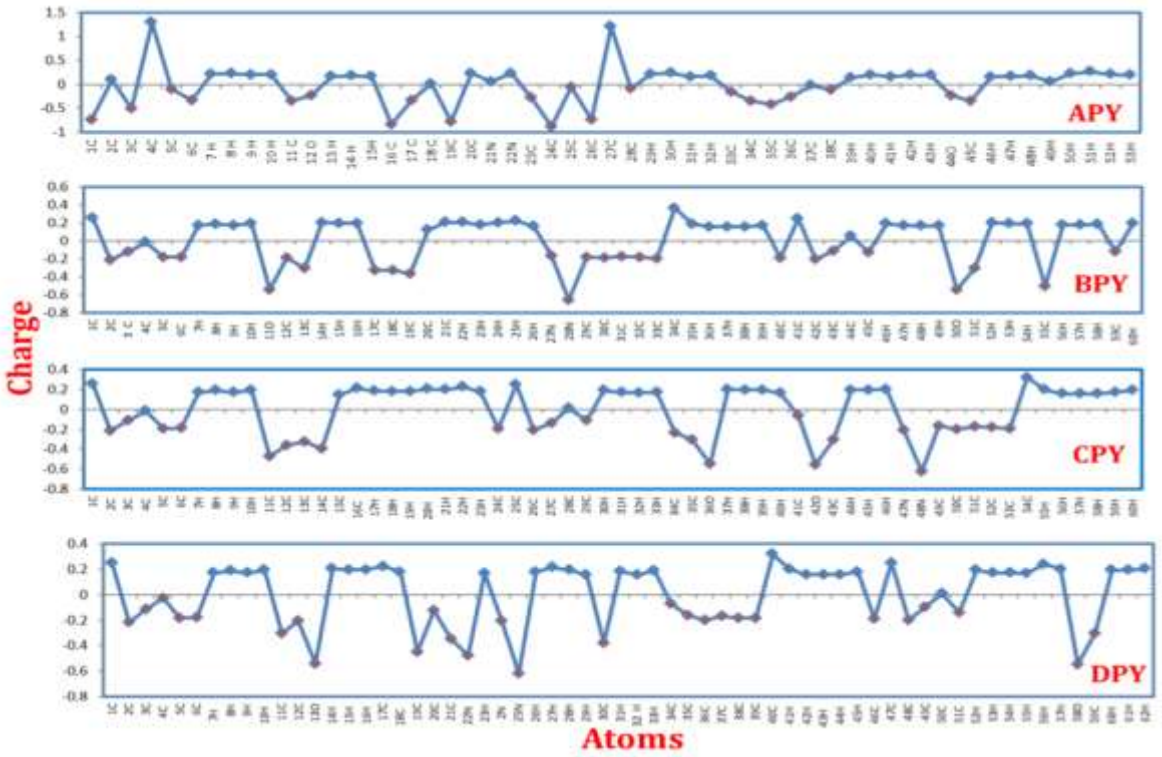

Figure 5. The atomic charge distribution according to Mulliken of Pyrazol MCC derivative (APY, BPY, CPY, and DPY).

Theoretical electronic absorption spectra of studied compounds

The time-dependent self-consistent field (TD-SCF) technique was used to evaluate the electronic spectra for B, C, BPY, and CPY compounds at the B3LYP/6-311G++ (d,p) theoretical level in ethanol to estimate the singlet excited states. The calculated excitation states, their oscillator strengths 〈f〉, and the measured electronic spectra for the analyzed compounds are shown in Table 1. The predicted absorption spectra obtained from the studied compounds have been shown in Figure 6. The electron transfer between HOMO and LUMO energy levels takes into consideration not only the transition energy, 〈ΔE〉, but also the strength of the oscillator 〈f〉. Most electronic transitions took place between the elevated HOMO levels and the lowered LUMO level, due to a small transition energy, 〈ΔE〉, between these two levels. Similarly, the 〈f〉 value indicated a highly significant probability of these transitions occurring. The system is unsaturated due to its properties, and thus there is a high correlation among π-π* transitions, resulting in an increased probability of active charge transfer. The TD-DFT of B, C, BPY and CPY exhibited notable electronic transitions at visible and ultraviolet regions. In addition, compound BPY showed the greatest absorption wavelength (λmax = 430.89 nm) and the lowest transition energy gap (2.8774 eV) corresponding to enhanced electronic delocalization and enhanced intramolecular charge transfer across the molecular structure. Compounds B and C exhibited absorption bands close to 416.97 and 414.32 nm,

respectively, which were attributed to the HOMO→LUMO transition, yielding values above 88%, supporting the dominant π→π* electronic excitation as their high oscillator strength (f) values indicated. Weak transitions were also observed for these compounds during excitation from H−1 and H−2 orbitals to the LUMO or from HOMO to LUMO+1, which suggested that more than one molecular orbital was involved in the higher excited state. Compound CPY showed a blue shift with the shorter wavelength (396.69 nm) in comparison with BPY with an energy gap of 3.1254 eV, likely due to a reduced conjugation efficiency in comparison to BPY. Relative high oscillator strength values reported for each B, C, BPY and CPY compound indicate good electronic absorption behaviour and also that an efficient electronic transition was realized in the conjugated system. It was found that a pyrazole moiety added showed the electronic structure and spectral response of them were adjusted, revealing the important structural modification in tuning the optoelectronic properties of the studied compounds.

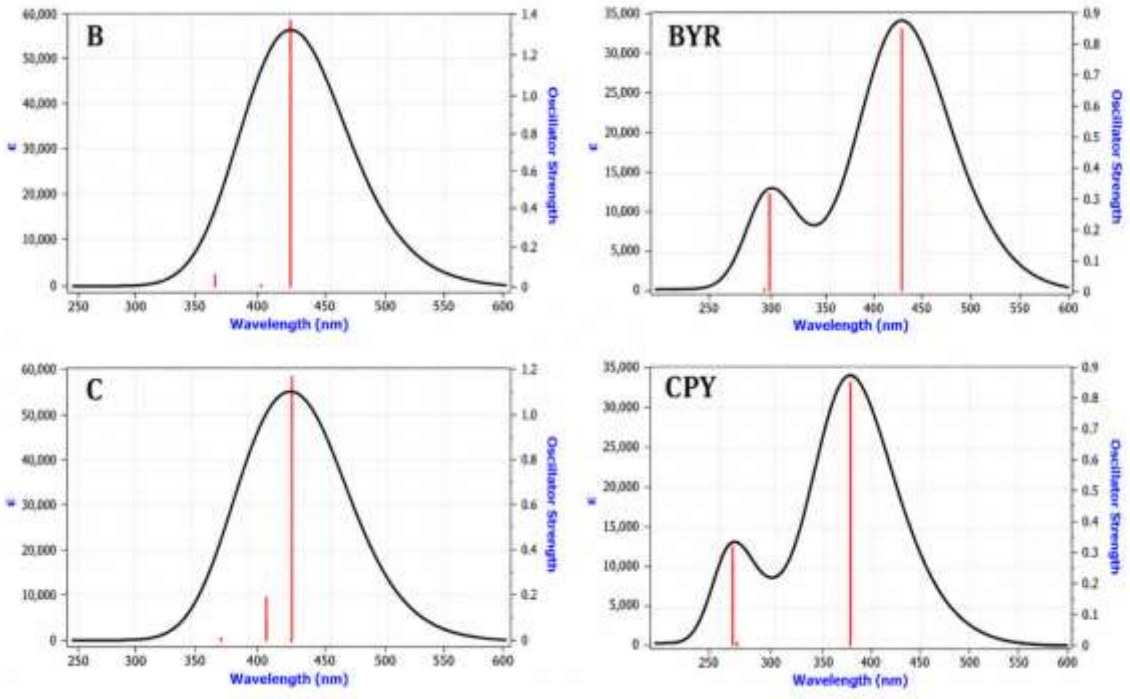

Figure 6. The theoretical electronic spectra of B, C, BPY and CPY compounds

The frontier molecular orbitals (FMO) analysis

Frontier molecular orbital (FMO) analysis was applied to compounds A, B, C, D and their pyrazole derivatives APY, BPY, CPY, and DPY based on the measured HOMO and LUMO energy values in order to analyze the electronic characteristics, the charge transfer modes, and the chemical reactive properties. The measured HOMO energies of compounds A, B, C and D were −0.2226, −0.2134, −0.2195 and −0.2215 a.u., respectively, as were LUMO energies of −0.0998, −0.0846, −0.0931 and −0.0948 a.u.; respectively the energy gap (ΔE = ELUMO − EHOMO) was 0.1227, 0.1287, 0.1263 and 0.1267 a.u (Figure 7). Compound A shows the lowest energy gap, reflecting higher chemical reactivity and easier intramolecular charge transfer than the other monocarbonyl curcumin analogues;

in contrast, compound B has the highest HOMO energy and larger energy gap, indicating relatively lower electronic softness and higher kinetic stability. For the pyrazole derivatives APY, BPY, CPY, and DPY, which were determined to have HOMO energies −0.1941, −0.1789, −0.1950, and −0.1843 a.u. respectively, compared to the energy gap for LUMO energies −0.0629, −0.0627, −0.0609, and −0.0557 a.u. In relation to pyrazole derivatives, BPY exhibited the lowest ΔE value (0.1162 a.u.), reflecting higher electronic delocalization, more favorable softness, and improved rate of charge transfer. In contrast, CPY was found to have the highest energy gap (0.1341 a.u.) (Figure 8), which indicates increased stability and reduced chemical reactivity. The distributions of HOMO of most compounds were found to be predominantly on the bound regions of the conjugated π-system and aromatic rings which would be considered the electron donating site. In contrast, the LUMO orbitals were oriented along electron-accepting conjugated fragments, indicating that electronics are mostly linked to π→π* transitions of internal electron transfer. The orbitals of the pyrazole derivatives show that with the inclusion of the pyrazole moiety electronic structure undergoes significant changes and the power exchange within the molecules increases. The smaller the gap of energy between the two HOMO–LUMO, the higher the polarizability, the lower the excitation energy and the better the chance of having an electronic transition. Thus, compounds A and BPY might show higher electronic and optical activity with their lower ΔE properties. On the other hand, larger band gap compounds like CPY are predicted to have increased stability and decreased reactivity. The FMO results demonstrate clearly that the functional structure modification by pyrazole ring formation can lead to significantly different electronic properties for the investigated compounds and regulate the reactivity and intramolecular charge-transfer properties of the studied compounds.

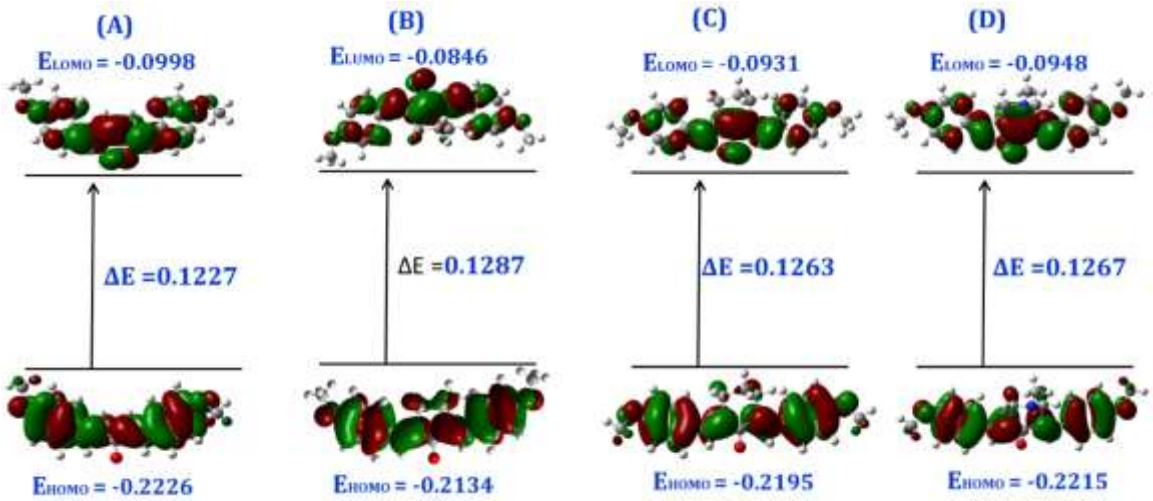

Figure 7. Frontier molecular orbital (FMO) of A, B, C, and D MCC compounds

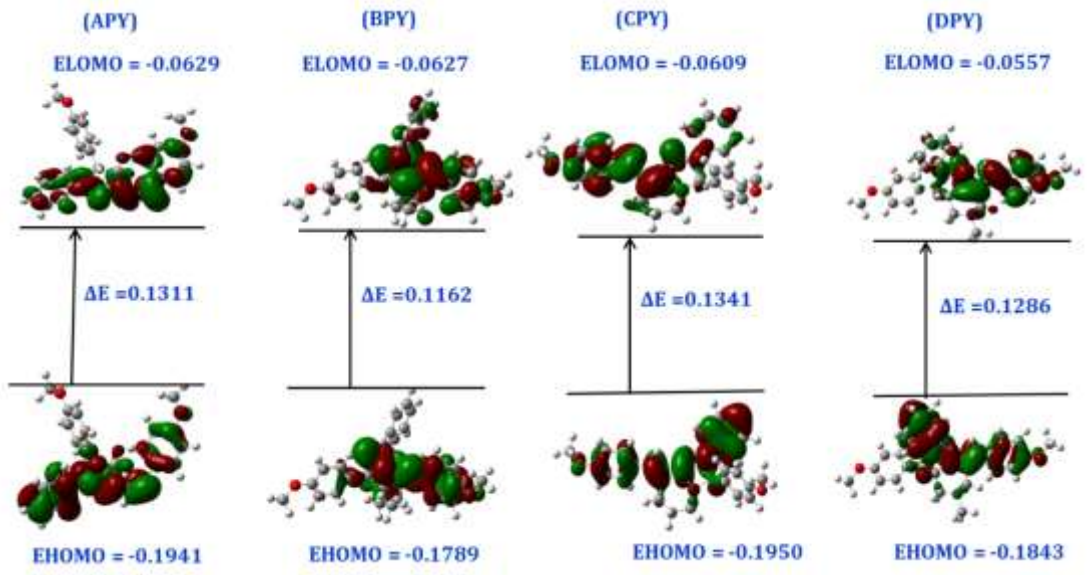

Figure 8. Frontier molecular orbital (FMO) of APY, BPY, CPY, and DPY MCC derivatives

Table 1. Theoretical band maxima and intensities and transition levels of studied compounds by using B3LYP/6-311G++(d,p).

Compound	Calculated λ_{max} (nm)	Transition energy gap (eV)	*f*	Contributions
B	416.97 394.53 357.8	2.9735 3.1426 3.446	1.3856 0.0011 0.0553	H->L (99.8 %) H-2 -> L (94.3%), H-1 -> L (3.792%) H-2 -> L (3.83%), H-1 -> L(93.34%) , H -> L+1(2.44%)
C	414.32 397.6 366.5	2.992 3.117 3.382	1.178 0.201 0.0049	H-2 -> L (10.95%), H->L (88.17%) H-2 -> L (86.32%) , H->L (11.32%) H-1 -> L (97.91%)
BPY	430.89 321.56 314.95	2.8774 3.8557 3.9367	0.8458 0.3204 0.0006	H->L (98.84 %) H-2 -> L (8.569%), H-1 -> L(87.62%)

Compound	Calculated λ_{max} (nm)	Transition energy gap (eV)	*f*	Contributions
				H-2 -> L (3.97%), H-> L+1(94.39%)
CPY	396.69	3.1254	0.8398	H->L (98.98 %)
	307.84	4.0276	0.0001	H-1 -> L (4.68%), H -> L+1 (93.24%)
	304.09	4.0276	0.3148	H-2 -> L (6.33%), H-1 -> L(80.95%) , H -> L+1(4.45%)

CONCLUSION

Fundamental Finding:

a. The molecular geometry of MCC was well established from its structure analysis where MCC compounds had approximately planar structure for geometry optimization, but if pyrazoles were added a non-planar arrangement can arise.
b. Mulliken charge identification and ESP mapping indicated that oxygen and nitrogen heteroatoms are the main electron-rich centers.
c. Pyrazole replacement helps to better separate the charge and delocalize electrons.
d. A lower energy gap than MCCs, reflected on the basis of frontier molecular orbital analysis, suggests higher chemical reactivity.
e. BPY exhibits the best electronic softness and intramolecular charge transfer efficiency among pyrazole derivatives.
f. Electronic transitions dominated by π-π* excitations, TD-DFT calculations.
g. Structural modifications, including addition of the pyrazole moiety, are successful in tuning optoelectronic response and absorption wavelengths.

Implication:

a. Modulation of the functional structure with the generation of ring structures from the pyrazole product plays a powerful role in controlling the reactivity, stability, and intramolecular charge transfer properties of monocarbonyl curcumin analogues.
b. The study provides guidance for designing more stable and biologically active curcumin-based heterocyclic systems.
c. Improved charge separation and delocalization can enhance chemical reactivity and optical properties for practical applications.

Limitation:

a. No explicit experimental validation is presented; the study relies on theoretical DFT and TD-DFT calculations.

b. Structural modifications and their effects are limited to the investigated MCC and pyrazole derivatives; generalization to other analogues is not confirmed.
c. Availability of data is conditional, as datasets require request from the corresponding author.

Future Research:

a. Experimental synthesis and validation of pyrazole-substituted MCC compounds to confirm theoretical predictions.
b. Investigation of other heterocyclic modifications to explore broader structure-property relationships.
c. Study of practical applications in optoelectronic devices or biological systems based on the tuned properties of these compounds.

REFERENCES

[1] B. B. Aggarwal and K. B. Harikumar, "Potential Therapeutic Effects of Curcumin," *Int. J. Biochem. Cell Biol.*, vol. 41, pp. 40–59, 2009.
[2] P. Anand, S. G. Thomas, A. B. Kunnumakkara, et al., "Biological Activities of Curcumin and Its Analogues," *Biochem. Pharmacol.*, vol. 76, pp. 1590–1611, 2008.
[3] S. J. Hewlings and D. S. Kalman, "Curcumin: A Review of Its Effects on Human Health," *Foods*, vol. 6, p. 92, 2017.
[4] S. C. Gupta, S. Patchva, and B. B. Aggarwal, "Therapeutic Roles of Curcumin," *AAPS J.*, vol. 15, pp. 195–218, 2013.
[5] V. P. Menon and A. R. Sudheer, "Antioxidant and Anti-inflammatory Properties of Curcumin," *Adv. Exp. Med. Biol.*, vol. 595, pp. 105–125, 2007.
[6] G. Liang, L. Shao, Y. Wang, et al., "Exploration and Synthesis of Curcumin Analogues with Improved Stability," *Bioorg. Med. Chem.*, vol. 17, pp. 2623–2631, 2009.
[7] K. I. Priyadarsini, "The Chemistry of Curcumin: From Extraction to Therapeutic Agent," *Molecules*, vol. 19, pp. 20091–20112, 2014.
[8] Y. J. Wang, M. H. Pan, A. L. Cheng, et al., "Stability of Curcumin in Buffer Solutions," *J. Pharm. Biomed. Anal.*, vol. 15, pp. 1867–1876, 1997.
[9] D. Shetty, Y. J. Kim, H. Shim, and J. P. Snyder, "Monocarbonyl Curcumin Mimics," *Molecules*, vol. 20, pp. 249–292, 2015.
[10] G. Liang, S. Yang, H. Zhou, et al., "Synthesis and Biological Evaluation of Monocarbonyl Analogues," *Eur. J. Med. Chem.*, vol. 44, pp. 915–919, 2009.
[11] K. M. Youssef, M. A. El-Sherbeny, F. S. El-Shafie, et al., "Synthesis and Biological Evaluation of Curcumin Analogues," *Arch. Pharm. Res.*, vol. 27, pp. 8–16, 2004.
[12] S. Vogel, M. Barbic, G. Jürgenliemk, and J. Heilmann, "Synthesis and Bioactivity of Curcumin Derivatives," *J. Nat. Prod.*, vol. 73, pp. 635–641, 2010.
[13] X. Qiu, Y. Du, B. Lou, et al., "Synthesis and Biological Evaluation of Curcumin Analogues," *Eur. J. Med. Chem.*, vol. 45, pp. 5302–5308, 2010.
[14] S. Fustero, M. Sánchez-Roselló, P. Barrio, and A. Simón-Fuentes, "Pyrazole Derivatives in Medicinal Chemistry," *Chem. Rev.*, vol. 111, pp. 6984–7034, 2011.
[15] A. Ansari, A. Ali, M. Asif, and Shamsuzzaman, "Review on Pyrazole Derivatives," *New J. Chem.*, vol. 41, pp. 16–41, 2017.

[16] K. Karrouchi, S. Radi, Y. Ramli, et al., "Synthesis and Pharmacological Activities of Pyrazole Derivatives," *Molecules*, vol. 23, p. 134, 2018.

[17] Y. Bansal and O. Silakari, "The Therapeutic Journey of Pyrazole Derivatives," *Bioorg. Med. Chem.*, vol. 20, pp. 6208–6236, 2012.

[18] J. Elguero, *Comprehensive Heterocyclic Chemistry II: Pyrazoles*. Oxford: Elsevier, 1996.

[19] U. V. Baviskar, et al., "Pyrazole-Incorporated Monocarbonyl Curcumin Analogues," *Polycycl. Aromat. Compd.*, vol. 45, pp. 1807–1836, 2025.

[20] P. Chaudhary, et al., "SAR Studies of Monocarbonyl Curcumin Analogues," *Curr. Org. Synth.*, vol. 20, pp. 821–837, 2023.

[21] Y. Li, J. Xu, and M. Zhang, "Theoretical Analysis of Monocarbonyl Curcumin Analogues," *Polycycl. Aromat. Compd.*, vol. 44, pp. 1918–1936, 2024.

[22] M. Clariano, et al., "Monocarbonyl Analogs of Curcumin," *Chem. Biodivers.*, vol. 20, p. e202300222, 2023.

[23] A. Brown, et al., "Monocarbonyl Curcumin Analogues as Anticancer Agents," *J. Med. Chem.*, vol. 56, pp. 3456–3466, 2013.

[24] A. D. Becke, "Density-Functional Thermochemistry III," *J. Chem. Phys.*, vol. 98, pp. 5648–5652, 1993.

[25] R. G. Parr and W. Yang, *Density Functional Theory of Atoms and Molecules*. Oxford: Oxford University Press, 1989.

[26] M. J. Frisch, et al., *Gaussian 09 Revision D.01*. Wallingford, CT: Gaussian Inc., 2013.

[27] F. Jensen, *Introduction to Computational Chemistry*, 3rd ed. Wiley, 2017.

[28] K. Fukui, "Role of Frontier Orbitals in Chemical Reactions," *Science*, vol. 218, pp. 747–754, 1982.

[29] T. Koopmans, "Ordering of Wave Functions and Eigenenergies," *Physica*, vol. 1, pp. 104–113, 1934.

[30] P. Geerlings, F. De Proft, and W. Langenaeker, "Conceptual DFT," *Chem. Rev.*, vol. 103, pp. 1793–1874, 2003.

[31] R. S. Mulliken, "Electronic Population Analysis on LCAO-MO Molecular Wave Functions," *J. Chem. Phys.*, vol. 23, pp. 1833–1840, 1955.

[32] P. Politzer and J. S. Murray, "Molecular Electrostatic Potentials," *Theor. Chem. Acc.*, vol. 108, pp. 134–142, 2002.

[33] G. Scalmani and M. J. Frisch, "Continuous Surface Charge Polarizable Continuum Models," *J. Chem. Phys.*, vol. 132, p. 114110, 2010.

[34] M. J. Frisch, G. W. Trucks, H. B. Schlegel, et al., *Gaussian 09, Revision A.02*. Wallingford, CT: Gaussian Inc., 2009.

[35] C. Lee, W. Yang, and R. G. Parr, "Development of the Colle-Salvetti correlation-energy formula into a functional of the electron density," *Phys. Rev. B*, vol. 37, pp. 785–789, 1988.

[36] S. Abbas, et al., "Antitumor, biological and nonlinear optical activities of novel thiazolidines," *Photochem. Photobiol. Sci.*, vol. 24, no. 11, pp. 1889–1909, Nov. 2025, doi: 10.1007/s43630-025-00800-0.

[37] A. G. Swadi, Q. M. A. Hassan, T. A. Alsalim, et al., "Computational study of nonlinear optical properties of dihydropyridine analogue (1,4-DHP-CHO) using DFT method," *Opt. Quant. Electron.*, vol. 57, p. 286, 2025, doi: 10.1007/s11082-025-08211-2.

[38] U. J. Al-Hamdani, N. S. Nwyr, and T. A. Alsalim, "Examining the liquid crystalline Behaviour and DFT modelling of the various terminal substituents of newly synthesized schiff

base/ester benzothiazole compounds," *J. Mol. Struct.*, vol. 1353(2), p. 144726, 2026, doi: 10.1016/j.molstruc.2025.144726.

[39] Z. Hashim, Q. M. A. Hassan, T. A. Alsalim, H. A. Sultan, and C. A. Emshary, "Synthesis, spectral, and NLO studies of indol derivative bearing 1,2,4-triazole-3-thiol group," *Opt. Mater.*, vol. 153, p. 115582, 2024, doi: 10.1016/j.optmat.2024.115582.

[40] A. G. Faisal, Q. M. A. Hassan, T. A. Alsalim, H. A. Sultan, F. S. Kamounah, and C. A. Emshary, "Synthesis, optical nonlinear properties, and all-optical switching of curcumin analogues," *J. Phys. Org. Chem.*, vol. 35, no. 10, p. e4401, 2022, doi: 10.1002/poc.4401.

[41] A. G. Faisal, Q. M. A. Hassan, T. A. Alsalim, H. A. Sultan, F. S. Kamounah, C. A. Emshary, and K. A. Hussein, "Curcumin analogue: Synthesis, DFT and nonlinear optical studies," *Optik*, vol. 306, p. 171800, 2024, doi: 10.1016/j.ijleo.2024.171800.

Hayder S. Mahdi
University of Basrah, Iraq

***Tahseen A. Alsalim (Corresponding Author)**
University of Basrah, Iraq
Email: tahseen.alsalim@uobasrah.edu.iq